EGU2014-7019
European Geosciences Union
General Assembly 2014
27 April - 02 May 2014, Vienna, Austria

GRAIL Gravity Field Determination Using the Celestial Mechanics Approach

D. Arnold, S. Bertone, A. Jäggi, G. Beutler, H. Bock, U. Meyer, L. Mervart

Astronomical Institute, University of Bern, Bern, Switzerland

Introduction

To determine the gravity field of the Moon, the two satellites of the NASA mission GRAIL (Gravity Recovery and Interior Laboratory) were launched on September 10 2011 and reached their lunar orbits in the beginning of 2012 (Zuber et al., 2013). The concept of the mission was inherited from the Earth-orbiting mission GRACE (Gravity Recovery and Climate Experiment) in that the key observations consisted of ultra-precise inter-satellite Ka-band range measurements. Together with the one- and two-way Doppler observations from the NASA Deep Space Network (DSN), the GRAIL data allows for a determination of the lunar gravity field with an unprecedented accuracy for both the near- and the far-side of the Moon. The first official GRAIL gravity field models contain spherical harmonic (SH) coefficients up to degree and order 660 (Konopliv et al., 2013, Lemoine et al., 2013).

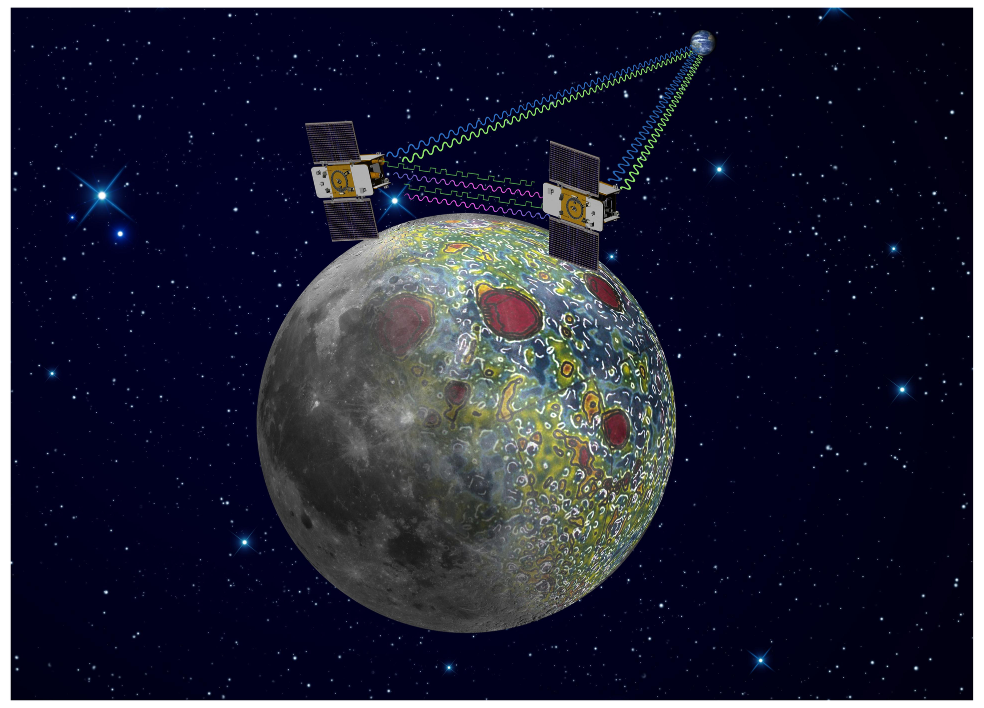

Copyright: NASA

Based on our experience in GRACE data processing, we are adapting our approach for gravity field recovery, the Celestial Mechanics Approach (CMA, Beutler et al., 2010), to the GRAIL mission within the Bernese GNSS software. We use the level-1b Ka-band range-rate (KBRR) data as original observations and - since the implementation of DSN data analysis into the Bernese GNSS software is still at the outset - the pre-processed reduced-dynamic GNI1B position data as pseudo-observations (relative weighting $10^8 : 1$). The following results are based on the release 3 data of the primary mission phase (1 March to 29 May 2012).

The Celestial Mechanics Approach (CMA)

The idea of the CMA is to rigorously treat the gravity field recovery as an extended orbit determination problem. It is a dynamic approach allowing for appropriately constrained stochastic pulses (instantaneous changes in velocity) to compensate for inevitable model deficiencies. For each satellite, the equations of motion to be solved read as $\ddot{\mathbf{r}} = \mathbf{a}_G + \mathbf{a}_P$, where $\mathbf{a}_G = \nabla V$ denotes the acceleration due to the gravity potential V, which we parametrize in terms of the standard SH expansion. $\mathbf{a}_P$ denotes the sum of all perturbing accelerations. We consider 3rd body perturbations according to JPL ephemerides DE421, forces due to the tidal deformation of the Moon and relativistic corrections. We do not yet model direct or indirect solar radiation pressure.
All observations contribute to one and the same set of parameters, which are simultaneously estimated. In our case, these are:

- Orbits: Initial conditions every 24h; once-per-revolution accelerations in R,S,W (radial, along-track, out-of-plane); stochastic pulses in R,S,W.
- Static gravity field: The coefficients of the SH expansion up to degree and order 200.
- Ka-band: Time bias every 24h.

Orbits

In a first step, we estimate a priori orbits using the GNI1B positions and KBRR observations. Fig. 1 shows that their quality strongly depends on the a priori gravity field used.

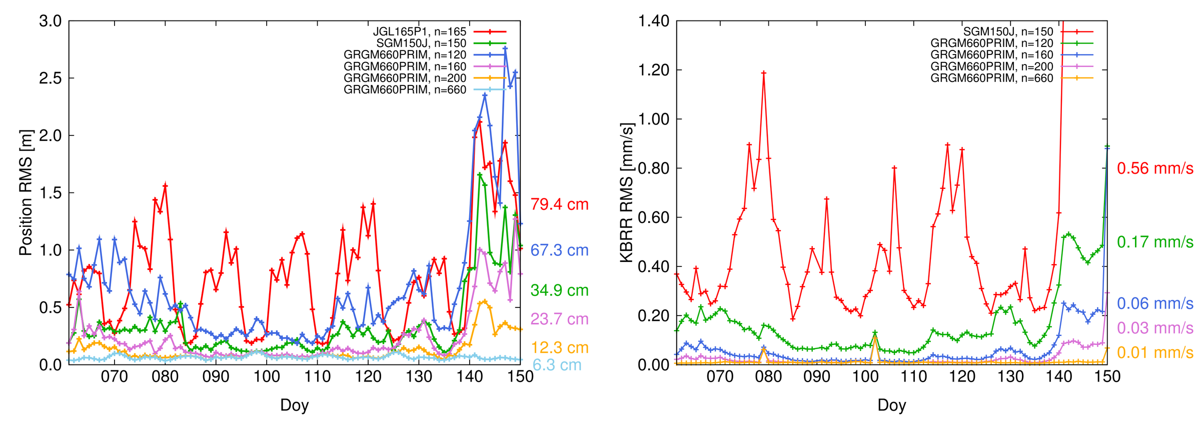

Figure 1: Left: RMS values of the GNI1B position fit. Right: RMS values of the KBRR residuals in the combined (position and Ka-band) orbit solution. The fits are relatively bad when using the Lunar Prospector (JGL165P1) or SELENE (SGM150J) gravity field and become better (more consistent) when introducing NASA's first official GRAIL field GRGM660PRIM (Lemoine et al., 2013), truncated at the degrees indicated.

Fig. 2 (left) shows Ka-band residuals for day 069. The gravity field GRGM660PRIM was used up to degree and order 660. Compared to the expected noise level of around 0.05 μm/s, the residuals are still relatively large and show clear once-per-revolution signals. The green and blue bars indicate the time spans during which each satellite is in sunlight. The obvious correlation between these time spans and the large residuals suggests that radiation pressure modeling is crucial. The residuals turn out much larger, if one does not allow for a Ka-band time bias, i.e. a shift in observation epoch between Ka-band and position observations. In the primary mission phase this bias is at around one second (see Fig. 2 right).

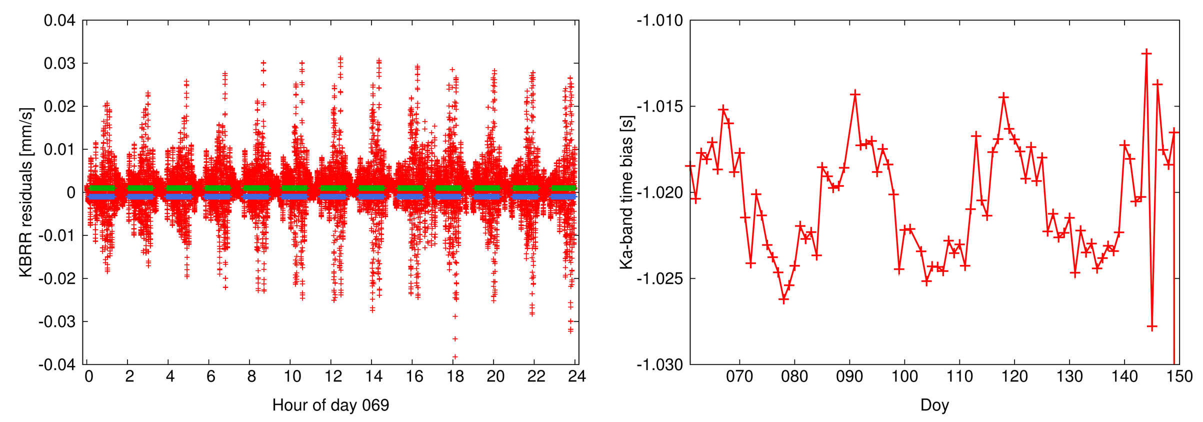

Figure 2: Left: KBRR residuals and time spans for which GRAIL-A (green) and GRAIL-B (blue) are in sunlight. Right: The estimated Ka-band time biases.

Gravity field

We set up stochastic pulses every 40 minutes. This value is a compromise between making up for model deficiencies and not absorbing too much of the gravity signal. Fig. 3 (left) shows the difference degree amplitudes (w.r.t. GRGM660PRIM) for different intervals between the stochastic pulses.

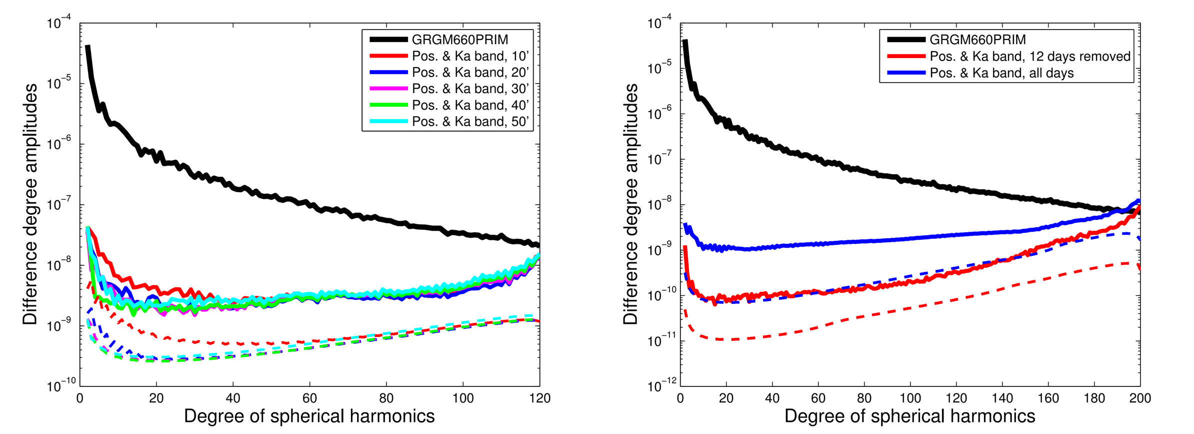

Figure 3: Difference degree amplitudes (solid) and formal errors (dashed). Left: The impact of the stochastic pulses. Right: Degree-200 solutions based on the a priori field GRGM660PRIM up to degree and order 200.

The orbits determined in the first step serve as a priori orbits for a common orbit and gravity field estimation on a daily basis. A classical least-squares adjustment is used. The daily normal equation systems (NEQs) are stacked to weekly, monthly and finally three-monthly NEQs, which are then inverted. Fig. 3 (right) shows the difference degree amplitudes of the degree-200 solution (a priori field was GRGMPRIM660 up to degree and order 200). The solution strongly improves when the data of 12 problematic days with larger residuals is completely skipped (blue vs. red curve). Data and residual screening still have to be refined to keep the maximum amount of data without degrading the solution. Fig. 4 shows the gravity anomalies of the degree-200 solution.

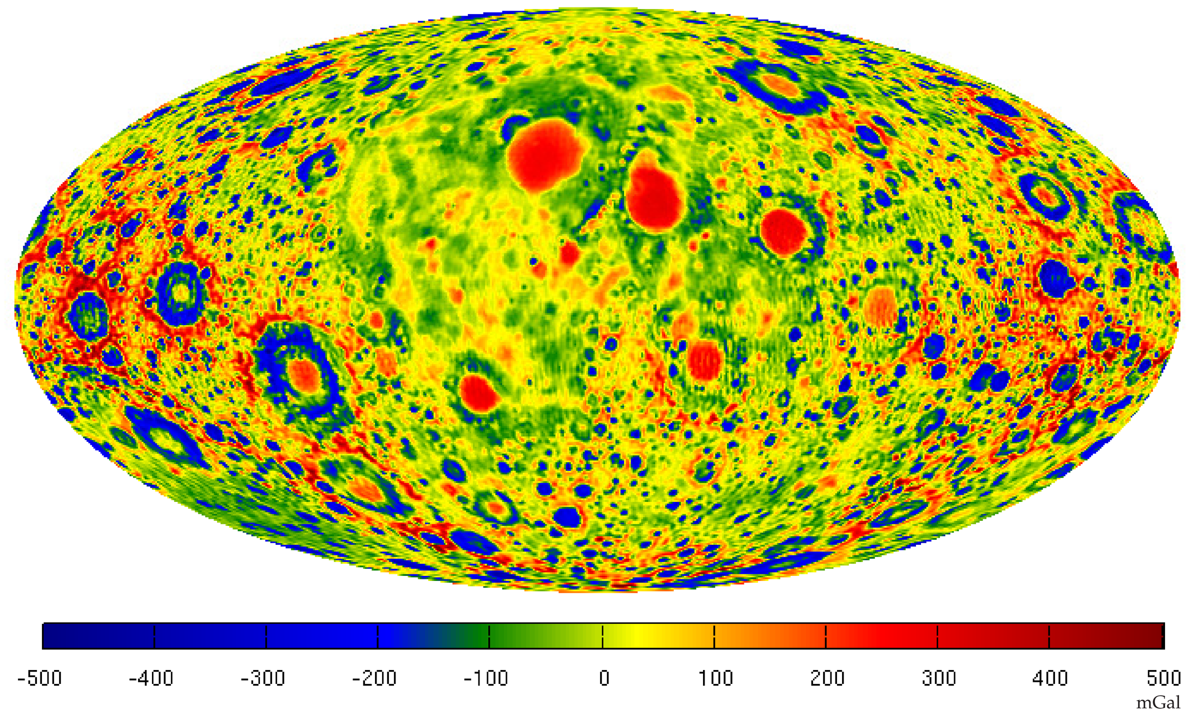

Figure 4: Free-air gravity anomalies of the degree-200 solution. Mollweide projection centered around meridian (nearside).

An important feature of the CMA is its relative insensitivity for the used a priori field. Fig. 5 shows difference degree amplitudes of solutions obtained with the indicated a priori fields. Already in the first iteration the SELENE field is improved basically to the same field as when starting with GRGM660PRIM up to degree and order 120. The Lunar Prospector field (much poorer on the far-side) leads to a comparable result after the second iteration.

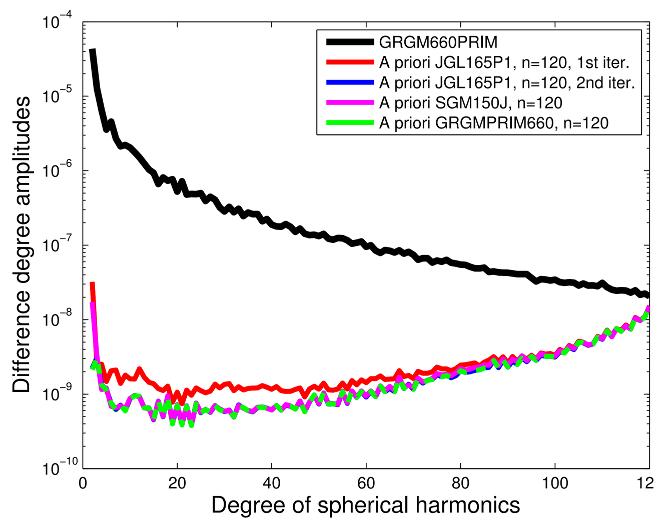

Figure 5: Difference degree amplitudes for solutions obtained with different a priori fields.

Doppler data processing

Besides the KBRR observations, GRAIL orbit and gravity field determination is based on its Doppler tracking by several Earth-based stations of the DSN. The basic signal is the frequency registered at the reception station based on cycles accumulated over a given time. In practice, Doppler observables are reconstructed from the travel time of a series of radio signals between the satellite and the DSN station over a given "counting interval" T_c (Moyer, 2000) as

$$\mathcal{D}_C = M_2 f_T(t) \frac{\rho_e - \rho_s}{T_c} ,$$

where $\mathcal{D}_C$ is the computed Doppler (C), ρ_s and ρ_e are precision light-time for the first and last signal of the series, M_2 is the spacecraft turnaround ratio (a constant scaling factor applied by the probe to the frequency of the tracking signal) and $f_T(t)$ is the transmitter frequency.

In order to process GRAIL Doppler observations, we then need an analytical model of light propagation including

- the trajectory of the tracking station and a GRAIL orbit (from a GNI1B position fit) in a common reference frame (we shall choose the Barycentric Celestial Reference System),
- a modeling of biases and non-geometrical effects in the Doppler signal (atmospheric delay, etc.) and the ephemeris of Solar System bodies (for relativistic effects).

The difference between the computed Doppler and the observed Doppler signal (O) registered at the DSN station constitutes the O-C term of the normal equation to be solved in the orbit determination process. We are currently improving the Doppler modeling in the Bernese GNSS software in order to reach the mm/s accuracy before undertaking the orbit determination process.

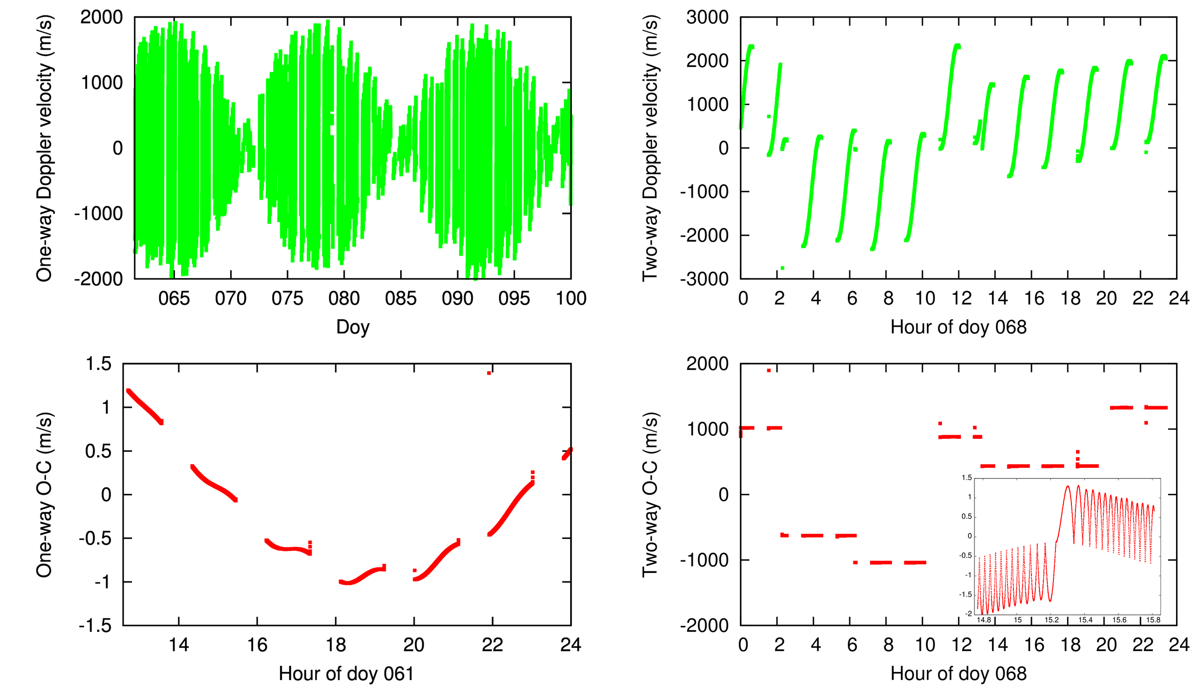

Figure 6: Current status of X-band one-way (left) and S-band two-way (right) Doppler observables for GRAIL in the Bernese GNSS software. Left: The upper plot shows the evolution of the observed one-way Doppler radial velocity over 3 months while in the lower we show our current O-C residuals over 1 day. Right: The upper plot shows the evolution of the observed two-way Doppler signal over 1 day (one can notice that several offsets are applied to the signal) while in the lower we show our current O-C residuals over 1 day ($\sim$ 1 m/s amplitude in each offset interval, see zoomed plot).

Conclusions

- The adaption of the CMA from GRACE to GRAIL allows for first lunar gravity fields obtained with the Bernese GNSS software.
- Further investigations are necessary to fully exploit the precision of the Ka-band observations. Both the force modeling (especially radiation pressure) and the data screening have to be refined.
- We are making progress in the implementation of DSN data analysis. More work is needed before DSN Doppler observations instead of the GNI1B products may be used for orbit and gravity field determination, which is necessary to obtain fully independent solutions.

References

Beutler et al. (2010) The celestial mechanics approach: theoretical foundations. J Geod 84:605-624 and The celestial mechanics approach: application to data of the GRACE mission. J Geod 84:661-681
Konopliv et al. (2013) The JPL lunar gravity field to spherical harmonic degree 660 from the GRAIL Primary Mission. J. Geophys. Res. Planets 118, 1415-1434
Lemoine et al. (2013) High-degree gravity model from GRAIL primary mission data. J. Geophys. Res. Planets 118, 1676-1698
Moyer (2000) Formulation for Observed and Computed Values of Deep Space Network Data Types for Navigation. JPL Publications
Zuber et al. (2013) Gravity field of the moon from the gravity recovery and interior laboratory (GRAIL) mission. Science, 339(6120), 668-671

Contact address

Daniel Arnold
Astronomical Institute, University of Bern
Sidlerstrasse 5
3012 Bern (Switzerland)
daniel.arnold@aiub.unibe.ch

Poster compiled by D. Arnold, April 2014
Astronomical Institute, University of Bern, Bern
daniel.arnold@aiub.unibe.ch